



# Automated determination of nitrite in aqueous samples with an improved integrated flow loop analyzer

Baomin Liu<sup>a,1</sup>, Haitao Su<sup>b,1</sup>, Shu Wang<sup>c</sup>, Zhen Zhang<sup>d</sup>, Ying Liang<sup>e</sup>, Dongxing Yuan<sup>c</sup>, Jian Ma<sup>c,\*</sup>

<sup>a</sup> State Key Laboratory of Marine Environmental Science, College of Ocean and Earth Sciences, Xiamen University, Xiamen, 361102, People's Republic of China

<sup>b</sup> School of Electronic Engineering and Automation, Guilin University of Electronic Technology, Guilin 541004, People's Republic of China

<sup>c</sup> State Key Laboratory of Marine Environmental Science, College of the Environment and Ecology, Xiamen University, Xiamen, 361102, People's Republic of China

<sup>d</sup> College of Ocean and Earth Sciences, Xiamen University, Xiamen, 361102, People's Republic of China

<sup>e</sup> School of Life and Environmental Sciences, Guilin University of Electronic Technology, Guilin, 541004, People's Republic of China

## ARTICLE INFO

### Article history:

Received 26 March 2016

Received in revised form 1 July 2016

Accepted 1 July 2016

Available online 1 July 2016

### Keywords:

Nitrite

Griess reaction

Loop flow analyzer

Light-emitting diode

Single chip microcomputer

## ABSTRACT

A compact loop flow analyzer was developed for automated determination of nitrite in aqueous samples based on Griess reaction and spectrophotometric detection. The integrated system employed a customized single chip microcomputer based hardware and laboratory-programmed software written by LabVIEW to control the injection valve, pumps and optical detection module. Experimental parameters related to nitrite analysis, including the reagent volume, sample temperature and salinity were evaluated and optimized. This fully automated analyzer showed a limit of detection as low as 0.02 μM with sample throughput of 15 h<sup>-1</sup>. The calibration curves prepared in pure water and low nutrient seawater were consistent over the linear range of 0–10 μM ( $R^2 = 0.999$ ), showing insignificant interference from the common ions in seawater. Different aqueous samples were successfully analyzed using both the present analyzer and the standard benchtop method, and the results from the two techniques showed no significant difference according to the statistical *t*-test ( $P = 0.95$ ). This compact automatic analyzer is simple, fully integrated, and user-friendly, making it highly suitable for field applications, such as on-line environmental monitoring and underway analysis.

© 2016 Elsevier B.V. All rights reserved.

## 1. Introduction

The nitrite plays an important role in various fields. For example, environmental scientists care about its toxicity to the environment and human health, therefore the US Environmental Protection Agency has set the maximum contaminant levels of nitrite in drinking water at 1 mg/L (21.7 μM) [1]; in the seawater, nitrite is an useful indicator for understanding the nitrification and denitrification processes in the marine nitrogen cycle, therefore nitrite concentration is considered as one of the basic nutrient data [2]; for analytical chemists, nitrite is a favorable testing analyte for newly developed analytical platforms, such as microfluidic paper-based analytical devices [3,4]. Therefore, the determination of nitrite is

of importance from environmental, oceanographical and analytical chemistry perspectives. When we searched the keywords "nitrite determination" in the database "Web of Science"; we found that the average number of annual publications on this topic was  $37 \pm 6$  from the year 2000 to 2015 (data shown as Fig. S1 in Supplementary Materials); which confirms that the determination of nitrite has received consistent attention from the scientific community over the years.

Reviews about nitrite analysis have been published [5,6], and the authors have summarized the different detection techniques, and discussed the advantages and limitations of the various methodologies. Very recently, several new techniques have been reported for nitrite detection, such as new electrodes [7], electrochemical sensors [8], capillary zone electrophoresis [9], high-resolution continuum source electrothermal molecular absorption spectrometry [10], fluorescent probes [11], quadruple isotope dilution mass spectrometry [12], etc. The most popular method for nitrite analysis is the spectrophotometric Griess assay, which is based

\* Corresponding author.

E-mail address: [jma@xmu.edu.cn](mailto:jma@xmu.edu.cn) (J. Ma).

<sup>1</sup> These two authors contributed equally.

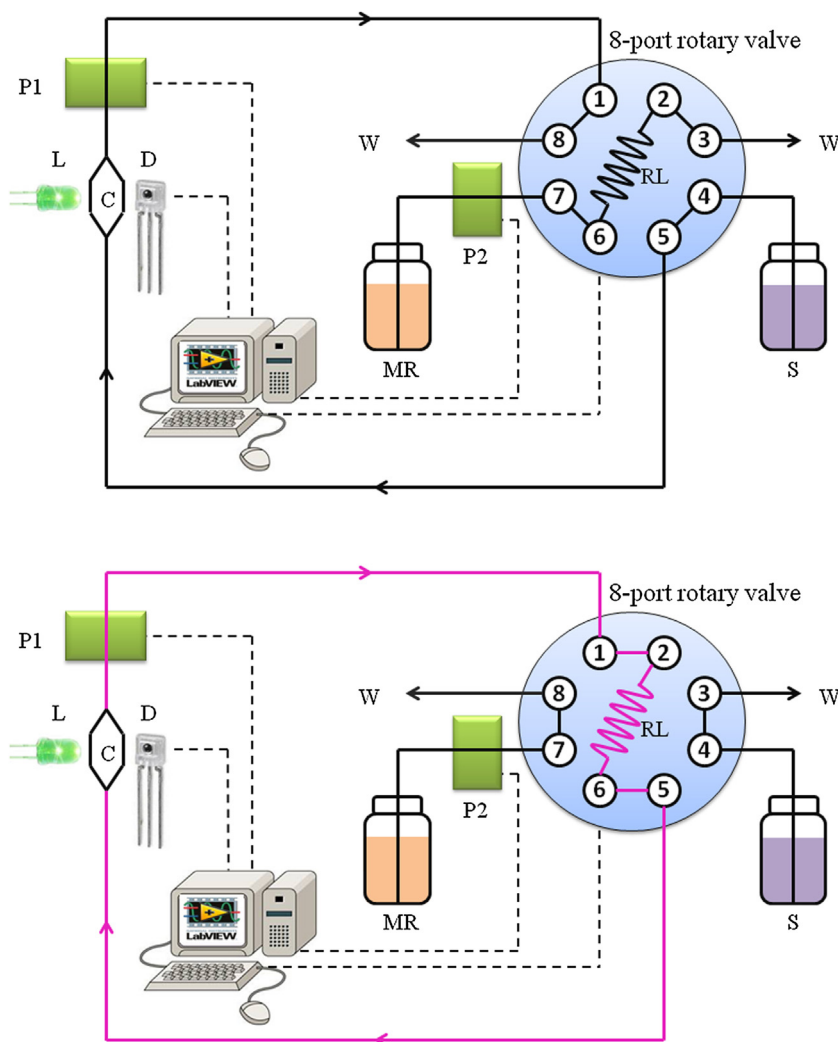


**Fig. 1.** Schematic diagram of the integrated loop flow analyzer (up: "Fill" position; down: "Inject" position). PP1/2: peristaltic pump 1/2; L: light source; C: cell; D: detector; W: waste; RL: reagent loop; MR: mixed reagent; S, sample. The volumes of reaction loop and sample loop are 75  $\mu$ L and ~3 mL, respectively.

on the diazotization of nitrite with sulfanilamide (SAM) and N-1-naphthylethylenediamine dihydrochloride (NED) under acidic conditions. The resulting pink-color azo dye can be detected at 540 nm [13]. The Griess reaction has been combined with different kinds of techniques to widen its application, such as microfluidic chip-based system [14,15], liquid core waveguide [16], solid phase extraction [17], etc. It should be noted that the flow analysis method combined with Griess reaction is still the mainstream or approved method for nitrite analysis [13].

The current flow based method suffers from problems caused by differences in refractive index of samples with various levels of salinity and the presence of incidentally formed bubbles, which can be major issues for the optical detection. Recently, we developed a loop flow analysis method for the determination of phosphate in aqueous samples using a novel cross-shaped flow cell, which was able to overcome these problems [18]. The principle of this method is that the optical path of the cell is perpendicular to the flow path (i.e. "cross-shaped"), therefore when the cell is positioned with horizontal light path and vertical liquid flow path, the bubbles in the cell can float away and be removed from the optical path [19]. Moreover, the reagent consumption of loop flow based system is less than some other flow analysis, and the steady state chemical condition is more reproducible under different circumstance. However, the previously described system utilized several individual

commercial instruments, and thus it was only suitable for bench-top use and too complicated for field application (data not shown). Therefore, we demonstrate here an integrated loop flow analyzer for nutrient monitoring, which is suitable for field applications. The developed analyzer has been optimized and different parameters were evaluated. This analyzer has been successfully applied for the determination of nitrite in different kinds of aqueous samples.

## 2. Experimental

### 2.1. Reagents

All chemicals used in this study were of reagent grade or higher quality, purchased from Sinopharm Chemical Reagent Co., China ([www.reagent.com.cn](http://www.reagent.com.cn)) and used without further purification. Nitrite stock solutions of 100 mM were prepared by dissolving pre-dried solid NaNO<sub>2</sub> in water. Working solutions of 400  $\mu$ M was prepared by stepwise dilution of the stock solutions with water. The SAM solution of 10 g/L was prepared by dissolving SAM in 10% HCl (v/v) solution, and the NED solution of 1 g/L was prepared by dissolving NED in water. The working reagent solution was a 1:1 mixture of SAM and NED solutions. All the standard and reagent solutions were stored at 4 °C in a refrigerator while not in use.

**Table 1**

The descriptions of the proposed loop flow analysis program.

Step	Time, s	P1 flow rate, mL/min	P1 direction	P2 flow rate, mL/min	P2 direction	Valve position	Description
1	50	15	Clockwise	2	Clockwise	Fill	Adding new sample into sample loop and flushing out the residual of last sample; filling the reagent loop, spectrophotometer setting zero (100% T)
2	30	9.0	Counter Clockwise	0	-	Inject	Sample and reagent mixing
3	150	0	-	0	-	Inject	Waiting for formation of azo dye, data recording

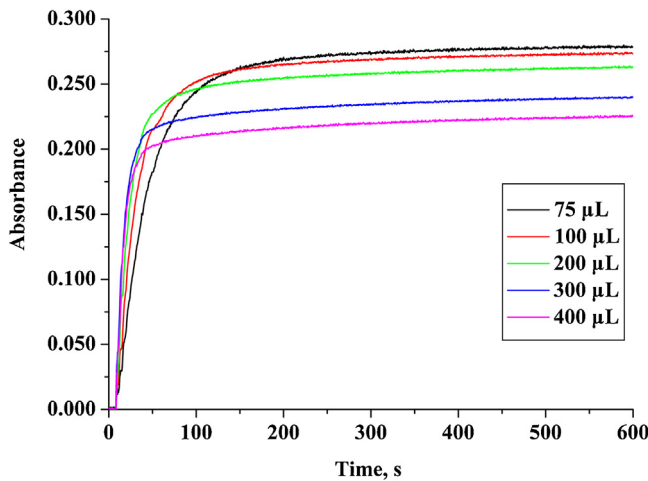


Fig. 2. Effect of reagent volume on signal with tested sample concentration of 10  $\mu\text{M}$ .

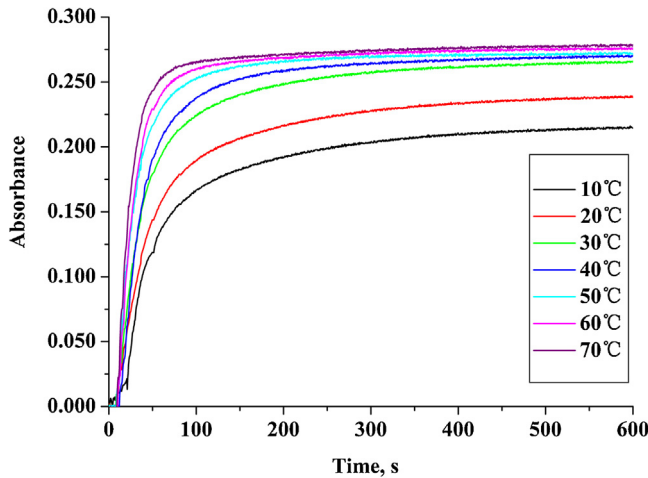


Fig. 3. Effect of sample temperature on signal with tested sample concentration of 10  $\mu\text{M}$ .

Pure water ( $18.2 \text{ M}\Omega \times \text{cm}$ ) obtained from a Millipore Purification System ([www.millipore.com](http://www.millipore.com)) was used throughout.

## 2.2. Apparatus

The loop flow manifold in this study is similar to that previously described for phosphate [18] and total alkalinity [19] analysis, however this new analyzer is more integrated and user-friendly as a portable instrument. As shown in Fig. 1, the loop flow analyzer utilized one eight-port injection valve (C22-3188EH, [www.vici.com](http://www.vici.com)), two low cost peristaltic pumps (BQ50-1J) equipped with 1 mm/2 mm i.d PVC tubing ([www.longerpump.com](http://www.longerpump.com)) for deliver-

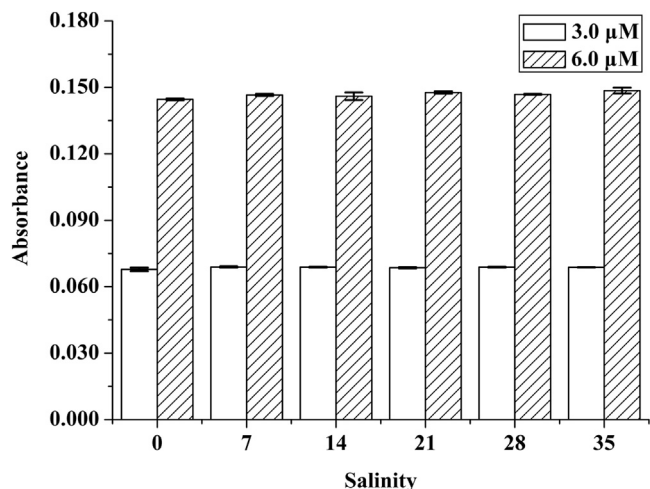
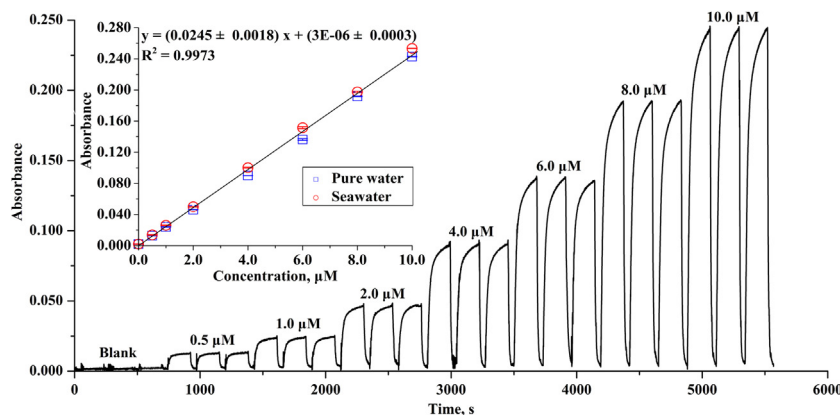


Fig. 4. Effect of sample salinity on the determination of samples.

ing reagent/sample, and an integrated laboratory-made detection and control system. The detection system included a 5 mm green light-emitting diode (LED,  $\lambda_{\text{max}} = 532 \text{ nm}$ , [www.cree.com](http://www.cree.com)), a light to voltage converter (TSL 257, [www.taosinc.com](http://www.taosinc.com)) and a customized cross-shaped flow cell (path length of 1.2 cm, volume of 1.5 mL). The emission spectra of LED and the absorption spectra of the formed Griess reaction product showed excellent agreement (Fig. S2). All the pump and valve switching processes and data acquisition were performed using a laboratory-programmed software written by LabVIEW ([www.ni.com](http://www.ni.com)) and single chip microcomputer (STM32F103VBT6, [www.st.com](http://www.st.com)) based hardware. The analyzer size is  $45 \text{ cm} \times 25 \text{ cm} \times 12 \text{ cm}$ , and the power consumption is  $\sim 12 \text{ W}$ . The detection system of LED-photodiode is very stable during the analysis procedure (absorbance variation of  $\sim 0.0002$ ). The detailed circuits of main board, devices driving and controlling are shown in the Supplemental Materials (Fig. S3–S6). PTFE tubing of 0.8 mm i.d. ([www.vici.com](http://www.vici.com)) was used as the fluid conduits throughout.

## 2.3. Analytical procedure

The analytical procedure has three steps as shown in Table 1. During step 1, new sample and fresh reagent were introduced to the sample and reagent loops, respectively. When the cell was filled with fresh sample, the detector was set to zero (100% transmittance). In the next step, the valve was switched from "Fill" to "Inject" position, which resulted in these two loops forming a whole loop, where sample and reagent would be mixed for 30 s. Finally, in step 3, both pumps were stopped and the formed pink azo dye was monitored and the absorbance data were shown by the software. All the steps were repeated until the procedure was stopped manually by the operator. It should be noted that in the preliminary experiments, it was determined that 50 s and 30 s were sufficient for



**Fig. 5.** Typical system signal output and calibration curves in pure water and seawater matrix (inset). Error bars are  $\pm$  standard deviation for triplicate analysis.

flushing the sample/reagent loop and mixing of sample and reagent, respectively (Fig. S7).

#### 2.4. Sampling

Low nutrient seawater was collected from the surface of the South China Sea and used as a matrix for salt-effect experiments. Lake water was collected from Furong Lake in the Xiang'an campus of Xiamen University. River water was collected from Jilong River. Coastal water was collected from Wuyuan Bay, Xiamen. These samples were filtered through a  $0.45\text{ }\mu\text{m}$  syringe type polyether sulfone filter immediately after collection. The filtered samples were kept at  $4^\circ\text{C}$  and analyzed within 24 h.

### 3. Results and discussion

#### 3.1. The effect of reagent loop

With a fixed reagent concentration, the reagent volume will determine the amount of reagent added to the sample. Therefore, the influence of reagent loop volume, from 50 to  $400\text{ }\mu\text{L}$ , was studied to determine the optimum value. Several typical output signals are shown in Fig. 2. With less reagent, the reaction was slow and took longer time to complete. On the other hand, with more reagent, the kinetic rate increased but the final result was lower because of the dilution effect from the reagent loop. Therefore,  $75\text{ }\mu\text{L}$  was chosen as the optimum volume of the reagent loop based on the balance of signal, reaction time and reagent consumption.

#### 3.2. The effect of sample temperature

The potential application of this analyzer is for field analysis on shipboard laboratories, where the collected samples will have various temperatures at different areas (from polar region to tropical area), depths (from surface to the deep ocean) and seasons (from summer to winter). Therefore, it is necessary to evaluate the effect

of sample temperature on the Griess reaction. For this purpose, the sample bottle was immersed in a water bath and the temperature was changed from  $10$  to  $70^\circ\text{C}$ . As shown in Fig. 3, it is obvious that higher temperature accelerates the reaction and shortens the analysis time. However, there are some potential risks in using high temperature for the reaction, such as the decomposition of organic nitrogen compounds, sample evaporation, and other consequences that might change the sample composition. Therefore, it is recommended to place the sample bottle in a water bath maintained at  $30$  or  $40^\circ\text{C}$  to keep the samples at constant temperature before analysis, especially for sample collected from cold areas (e.g. polar area).

#### 3.3. The effect of sample salinity

In order to apply this analyzer to underway analysis in coastal and estuary areas, it is necessary to study the effect of sample salinity on the results. Samples containing  $3$  and  $6\text{ }\mu\text{M}$  nitrite were prepared in water over a range of salinity levels ( $0$ – $35$ ) and analyzed as described in Section 2.3. As shown in Fig. 4, no significant salinity effect was found with this integrated LED-photodiode based optical detection system, which was in accordance with our previous study using commercial light source and detector [17]. The detector was set to zero (100% transmittance) when the cell was filled with a fresh sample at different salinity value, therefore the refractive index variance from the samples of different salinity values was corrected in the calculation.

#### 3.4. Analytical figures of merit

Fig. 5 shows the typical detector output for sample concentrations between  $0$  and  $10\text{ }\mu\text{M}$ . The sample throughput for the optimized conditions was  $15\text{ h}^{-1}$ . Standard curves prepared in pure water and low nutrient seawater are also shown in the inset of Fig. 5. The identical curves from both samples indicate that there is

**Table 2**  
Analytical results and recovery data of aqueous samples.

Sample type	Salinity	Concentration ( $n=3$ , $\mu\text{M}$ )		Calculated t-value	Critical t-value ( $P=0.95$ )	Spiked ( $\mu\text{M}$ )	Recovery (%)
		Flow method	Standard method				
Coastal water	18	$2.44 \pm 0.03$ (RSD = 1.2%)	$2.39 \pm 0.07$ (RSD = 2.8%)	1.33	2.78	5	105
Lake water	0	$0.81 \pm 0.01$ (RSD = 1.4%)	$0.83 \pm 0.04$ (RSD = 3.5%)	0.87	2.78	2	97.3
River water	0	$1.58 \pm 0.01$ (RSD = 0.3%)	$1.62 \pm 0.04$ (RSD = 2.2%)	1.8	2.78	3	98.6

no significant ionic strength effect and no specific ion effect from the major components of seawater.

The detection limit of the method was 0.02  $\mu\text{M}$ , which was calculated as three times the standard deviation for measurements of blank ( $n = 15$ ) divided by the slope of the calibration curve. The relative standard deviations for triplicate determinations of samples were 0.13–2.99% (Fig. 5), showing good reproducibility of the results at different sample concentrations.

### 3.5. Application

To evaluate the precision and accuracy of the developed analyzer, different water samples including river water, lake water and coastal water were analyzed using both this analyzer and the standard benchtop Griess assay. The results are tabulated in Table 2, and it can be seen that there is no statistically significant difference between the proposed and reference methods with the paired Student's *t*-test at the 95% confidence level. The spike recoveries were 97.3–105.0%, indicating little matrix interference in the determination of nitrite in different samples.

## 4. Conclusions

Compared with other flow mode, the combination of loop flow and "cross-shaped" flow cell showed the novelty of insignificant interference from salinity, free of the bubble problem and easier operation [18]. Therefore, a compact automatic loop flow analyzer has been developed and applied for the determination of nitrite in aqueous samples. The limit of detection was found to be 0.02  $\mu\text{M}$  with a short analysis time of ~4 min/sample. The precision and accuracy of the developed analyzer are more than satisfactory based on the highly reproducible recovery data and comparison results with the standard method. More importantly, the proposed analyzer can be easily modified for the determination of nutrients and other chemicals that are based on spectrophotometric detection. The more integrated design offers a simpler, lower cost and more user friendly method for nutrient analysis, and is highly suitable for field applications.

## Acknowledgements

This work was financially supported by the National Natural Science Foundation of China (41306090 and 41206077) and Xiamen Southern Oceanographic Center (14GST68NF32).

## Appendix A. Supplementary data

Supplementary data associated with this article can be found, in the online version, at <http://dx.doi.org/10.1016/j.snb.2016.07.002>.

## References

- [1] <http://www.epa.gov/your-drinking-water/table-regulated-drinking-water-contaminants>, (accessed 20.06.16).
- [2] J.A. Brandes, A.H. Devol, C. Deutsch, New developments in the marine nitrogen cycle, *Chem. Rev.* 107 (2007) 577–589.
- [3] T.M.G. Cardoso, P.T. Garcia, W.K.T. Coltro, Colorimetric determination of nitrite in clinical, food and environmental samples using microfluidic devices stamped in paper platform, *Anal. Methods* 7 (2015) 7311–7317.
- [4] N. Lopez-Ruiz, W.F. Curto, M.M. Erenas, F. Benito-Lopez, D. Diamond, A.J. Palma, L.F. Capitan-Vallvey, Smartphone-based simultaneous pH and nitrite colorimetric determination for paper microfluidic devices, *Anal. Chem.* 86 (2014) 9554–9562.
- [5] M.J. Moorcroft, J. Davis, R.G. Compton, Detection and determination of nitrate and nitrite: a review, *Talanta* 54 (2001) 785–803.
- [6] Y. Zhao, D. Zhao, D. Li, Electrochemical and other methods for detection and determination of dissolved nitrite: a review, *Int. J. Electrochem. Sci.* 10 (2015) 1144–1168.
- [7] H. Wang, P. Chen, F. Wen, Y. Zhu, Y. Zhang, Flower-like  $\text{Fe}_2\text{O}_3@\text{MoS}_2$  nanocomposite decorated glassy carbon electrode for the determination of nitrite, *Sens. Actuators B Chem.* 220 (2015) 749–754.
- [8] M. Parsaei, Z. Asadi, S. Khodadoust, A sensitive electrochemical sensor for rapid and selective determination of nitrite ion in water samples using modified carbon paste electrode with a newly synthesized cobalt(II)-Schiff base complex and magnetite nanospheres, *Sens. Actuators B Chem.* 220 (2015) 1131–1138.
- [9] F.D. Betta, L. Vitali, R. Fett, A.C.O. Costa, Development and validation of a sub-minute capillary zone electrophoresis method for determination of nitrate and nitrite in baby foods, *Talanta* 122 (2014) 23–29.
- [10] G.C. Brandao, G.D. Matos, R.N. Pereira, S.L.C. Ferreira, Development and a simple method for the determination of nitrite and nitrate in groundwater by high-resolution continuum source electrothermal molecular absorption spectrometry, *Anal. Chim. Acta* 806 (2014) 101–106.
- [11] L. Lu, C. Chen, D. Zhao, F. Yang, X. Yang, A simple and sensitive assay for the determination of nitrite using folic acid as the fluorescent probe, *Anal. Methods* 7 (2015) 1543–1548.
- [12] E. Pagliano, J. Mejia, Z. Mester, High-precision quadruple isotope dilution method for simultaneous determination of nitrite and nitrate in seawater by GCMS after derivatization with triethyloxonium tetrafluoroborate, *Anal. Chim. Acta* 824 (2014) 36–41.
- [13] J. Ma, L. Adornato, R.H. Byrne, D. Yuan, Determination of nanomolar levels of nutrients in seawater, *Trends Anal. Chem.* 60 (2014) 1–15.
- [14] J.-H. Ahn, K.H. Jo, J.H. Hahn, Standard addition/absorption detection microfluidic system for salt error-free nitrite determination, *Anal. Chim. Acta* 886 (2015) 114–122.
- [15] A.D. Beaton, V.J. Sieben, C.F.A. Floquet, E.M. Waugh, S.A.K. Bey, I.R.G. Ogilvie, M.C. Mowlem, H. Morgan, An automated microfluidic colourimetric sensor applied *in situ* to determine nitrite concentration, *Sens. Actuators B* 156 (2011) 1009–1014.
- [16] S. Feng, M. Zhang, Y. Huang, D. Yuan, Y. Zhu, Simultaneous determination of nanomolar nitrite and nitrate in seawater using reverse flow injection analysis coupled with a long path length liquid waveguide capillary cell, *Talanta* 117 (2013) 456–462.
- [17] M. Zhang, D. Yuan, Y. Huang, G. Chen, Z. Zhang, Sequential injection spectrophotometric determination of nanomolar nitrite in seawater by on-line preconcentration with HLB cartridge, *Acta Oceanol. Sinica* 29 (2010) 100–107.
- [18] J. Ma, Q. Li, D. Yuan, Loop flow analysis of dissolved reactive phosphorus in aqueous samples, *Talanta* 123 (2014) 218–223.
- [19] Q. Li, F. Wang, Z.A. Wang, D. Yuan, M. Dai, J. Chen, J. Dai, K. Hoering, Automated spectrophotometric analyzer for rapid sing-point titration of seawater total alkalinity, *Environ. Sci. Technol.* 47 (2013) 11139–11146.

## Biographies

**Baomin Liu** completed his Ph.D in 2008 from Xiamen University. He is an engineer in the platform of chromatography and mass spectrometry in the State Key laboratory of Marine Environmental Science at Xiamen University.

**Haitao Su** completed his Ph.D in 2015 from Xiamen University. He is an assistant professor in Guilin University of Electronic Technology with research interests of Electronic Engineering and Automation.

**Shu Wang** completed her Bachelor Degree in 2014 from Guangzhou University. She is a master student majoring in environmental science.

**Zhen Zhang** completed his Mater Degree in 2009 from Xiamen University. He is an engineer in the College of Ocean and Earth Sciences, Xiamen University, with research interests of marine chemistry and automatic instrumentation.

**Ying Liang** completed her Ph.D in 2006 from Xiamen University. She is a professor in Guilin University of Electronic Technology with research interests of analytical chemistry. Dr. Liang has published more than 20 papers and hosted several national funding.

**Dongxing Yuan** is a Professor at the State Key laboratory of Marine Environmental Science at Xiamen University since 1994. She earned her PhD from the University of Iowa in 1988 and was a Visiting Scholar at Perkin-Elmer (Uberlingen, Germany), Hong Kong University of Science and Technology and Texas A&M University. Her broad research interests are in environmental analytical chemistry, and specifically in metals and nutrients in seawater.

**Jian Ma** is an associate professor in Xiamen University. He got Ph.D in Xiamen University, 2008 and has postdoctoral experience (2009–2012) in University of Texas at Arlington and University of South Florida. His research interests include in field trace nutrient and metal analysis, flow analysis and automatic instrumentation. Dr. Ma has published 30 papers and hosted several national funding.